PAX6–WNK2 Axis Governs Corneal Epithelial Homeostasis

Liqiong Zhu,[1] Chaoqun Chen,[1] Siqi Wu,[1] Huizhen Guo,[1] Lingyu Li,[1] Li Wang,[1] Dongmei Liu,[1] Yu Zhan,[2] Xinyue Du,[1] Jiafeng Liu,[1] Jieying Tan,[1] Ying Huang,[1] Kunlun Mo,[1] Xihong Lan,[1] Hong Ouyang,[1] Jin Yuan,[1] Xiangjun Chen,[3,4] and Jianping Ji[1]

[1]State Key Laboratory of Ophthalmology, Zhongshan Ophthalmic Center, Sun Yat-Sen University, Guangdong Provincial Key Laboratory of Ophthalmology and Visual Science, Guangzhou, China
[2]Department of Experimental Research, Bioinformatics Platform, State Key Laboratory of Oncology in South China, Guangdong Provincial Clinical Research Center for Cancer, Sun Yat-Sen University Cancer Center, Guangzhou, China
[3]Eye Center of the Second Affiliated Hospital, Zhejiang University School of Medicine, Hangzhou, China
[4]Institute of Translational Medicine, Zhejiang University School of Medicine, Hangzhou, China

Correspondence: Hong Ouyang, State Key Laboratory of Ophthalmology, Zhongshan Ophthalmic Center, Sun Yat-Sen University, Guangdong Provincial Key Laboratory of Ophthalmology and Visual Science, Guangzhou 510060, China; ouyhong3@mail.sysu.edu.cn.
Jin Yuan, State Key Laboratory of Ophthalmology, Zhongshan Ophthalmic Center, Sun Yat-Sen University, Guangdong Provincial Key Laboratory of Ophthalmology and Visual Science, Guangzhou 510060, China; yuanjincornea@126.com.
Xiangjun Chen, Eye Center of the Second Affiliated Hospital, Zhejiang University School of Medicine, No. 1 West-Lake Avenue, Hangzhou 310009, China; chenxiangjun@zju.edu.cn.
Jianping Ji, State Key Laboratory of Ophthalmology, Zhongshan Ophthalmic Center, Sun Yat-Sen University, Guangdong Provincial Key Laboratory of Ophthalmology and Visual Science, Guangzhou 510060, China; jpji1974@126.com.

Received: April 2, 2024
Accepted: August 21, 2024
Published: October 25, 2024

Citation: Zhu L, Chen C, Wu S, et al. PAX6–WNK2 axis governs corneal epithelial homeostasis. *Invest Ophthalmol Vis Sci.* 2024;65(12):40. https://doi.org/10.1167/iovs.65.12.40

Purpose. Limbal stem/progenitor cells (LSCs) continuously proliferate and differentiate to replenish the corneal epithelium and play a vital role in corneal function and normal vision. A previous study revealed that paired box 6 (PAX6) is a master transcription factor involved in determining the fate of corneal epithelial cells (CECs). However, the molecular events downstream of PAX6 remain largely unknown. In this study, we aimed to clarify the regulation network of PAX6 in driving CEC differentiation.

Methods. An air–liquid culture system was used to differentiate LSCs into mature CECs. Specific targeting *PAX6* short-hairpin RNAs were used to knock down *PAX6* in LSC. RNA sequencing (RNA-seq) was used to analyze *shPAX6*-transfected CECs and CEC differentiation-associated genes to identify the potential downstream targets of PAX6. RNA-seq analysis, quantitative real-time PCR, and immunofluorescence staining were performed to clarify the function of WNK lysine deficient protein kinase 2 (WNK2), a downstream target of PAX6, and its relationship with corneal diseases.

Results. WNK2 expression increased during CEC differentiation and decreased upon *PAX6* depletion. The distribution of WNK2 was specifically limited to the central corneal epithelium and suprabasal layer of the limbus. Knockdown of *WNK2* impaired the expression of CEC-specific markers (KRT12, ALDH3A1, and CLU), disrupted the corneal differentiation process, and activated the terms of keratinization, inflammation, and cell proliferation, consistent with *PAX6*-depleted CEC and published microbial keratitis. Thus, aberrant expression of WNK2 was linked to corneal ulcers.

Conclusions. As a downstream target of PAX6, WNK2 plays an essential role in corneal epithelial cell differentiation and maintenance of corneal homeostasis.

Keywords: WNK2, corneal epithelial cell differentiation, corneal homeostasis

Nonkeratinized, stratified corneal epithelial cells (CECs) form the outermost cell layer of the cornea. Their integrity and homeostasis are essential for the maintenance of normal vision.[1,2] Limbal stem/progenitor cells (LSCs), the sole stem cell source of CECs, govern CEC replenishment and corneal wound healing.[3] During corneal epithelial cell turnover, LSCs divide into new LSCs and transient amplifying cells, which then migrate centripetally and gradually differentiate into mature CECs.[4–6] CEC differentiation and regeneration are fundamental for maintaining the physiolog-

ical functions of corneal epithelial cells and protecting them against pathogens. Mechanical and chemical ocular injuries or genetic mutations can impair LSC proliferation and differentiation, leading to persistent corneal epithelial defects, invasion of conjunctival cells, aberrant skin-like epithelial cell fate transition, and eventually blindness.[7,8]

Paired box 6 (PAX6) is a crucial transcription factor for developmental regulation of multiple ocular tissues, including the neuroretina, lens, anterior eye segment, and cornea. *PAX6* mutation or dosage reductions lead to aniridia and small eyes in both humans and mice.[9] PAX6 is widely expressed in the corneal epithelium, and it is required for LSC proliferation and CEC migration during corneal development.[10,11] Our previous study showed that PAX6 governs corneal epithelial cell fate determination and CEC differentiation. Diminished PAX6 expression transforms functional LSC into skin-like epithelium.[12] However, the molecular events leading to PAX6-mediated CEC differentiation remain unclear.

WNK lysine deficient protein kinase 2 (WNK2) is one of the four subfamilies of WNK protein kinases and encodes the expression of cytoplasmic serine–threonine kinase.[13] WNK2 was first discovered as a regulator of ion transport.[14] The expression of this protein is found in multiple tissues, such as the brain, small intestine, colon, and heart muscle. WNK2 can function as a tumor suppressor via the MEK1/ERK1/2 MAP kinase pathway.[15,16] It is also found to participate in the regulation of neuronal cation–chloride cotransporters and autophagy.[17,18] However, the role of WNK2 in corneal epithelium has not been reported.

In the present study, we found that WNK2 acts as a novel downstream factor of PAX6 in CECs. WNK2 promotes CEC maturation and suppresses cell proliferation. PAX6 triggers CEC differentiation and maintains corneal homeostasis via the PAX6–WNK2 axis. Decreased expression of WNK2 is closely associated with human corneal ulcer disease. Our findings provide a deeper understanding of the PAX6 downstream regulatory network in CECs and suggest that WNK2 can serve as a potential new regulator for CEC differentiation.

Materials and Methods

Samples and Cell Culture

Primary LSCs were obtained from human corneoscleral rims, which were supported by the eye bank of the Zhongshan Ophthalmology Center, Guangzhou, China (2023KYPJ126). All the experiments were done according to the ethics statement of the Ethics Committee of Zhongshan Ophthalmic Center.

Primary cultured LSCs were generated as follows: the corneoscleral rims were mechanically cut into 2-mm × 2-mm small pieces and incubated with 0.2% collagenase IV digestion solution (Gibco, Waltham, MA, USA; cat. 17104019) for 2 hours at 37°C. To obtain a single-cell suspension, the cell solution should be placed in 0.25% trypsin-EDTA (Gibco; cat. 25200072) solution for further digestion for 15 minutes at 37°C. After this step, the cells were collected and seeded in 2% Matrigel-coated (BD Bioscience, Franklin Lakes, NJ, USA; cat. 354230) polystyrene culture plates for primary LSC culture. The LSC culture medium was prepared as our previous work described[12] and was changed every 2 days until cell confluence. The reagents information is shown in Supplementary Table S1.

CEC Differentiation Assay

LSC-derived CECs were cultured using an air–liquid differentiation system. Briefly, the transwell insert was coated with 30 µg/mL collagen I. Next, approximately 2.5 × 10^5 LSCs were seeded in each transwell insert. For the first stage, cells were cultured in LSC medium and changed every other day until they reached 100% confluence, which was essential for supporting the cell differentiation process in the next step. At the CEC differentiation stage, the medium in the upper insert was aspirated, while the medium in the lower insert was replaced by CEC medium and the volume was reduced to 200 µL per insert. During the differentiation period, the upper insert remained empty and the medium in the lower insert was changed every day for 5 days to obtain mature CECs. The CEC medium was composed of Dulbecco's modified Eagle's medium/F12 medium supplemented with 10 ng/mL cholera toxin (Sigma-Aldrich, St. Louis, MO, USA; cat. C8052), 50 nM retinoic acid (Tocris, Bristol, UK; cat. 0695), 1.2 mM calcium chloride (Sigma-Aldrich), 10 ng/mL KGF (MedChemExpress, Hong Kong, China; cat. HY-P70673), 10% knockout SR serum replacement (Gibco; cat. 10828-028), and 1% penicillin–streptomycin.

Hematoxylin and Eosin and Immunofluorescence Staining

Cell samples were fixed with 4% paraformaldehyde at room temperature for 30 minutes before staining procedures. Human corneoscleral rims (tissues for normal corneal sections), human corneal ulcer tissues, and CEC cell sheets were fixed with 10% neutral-buffered formalin solution. Tissues were fixed for 30 minutes at room temperature. CEC cell sheets were fixed overnight at 4°C, followed by their placement in the histogel (Thermo Fisher Scientific, Waltham, MA, USA, cat. R904012). After dehydration, samples were paraffin embedded and cut into 5-µm sections. Before staining, all paraffin samples were deparaffinized.

For hematoxylin and eosin (H&E) staining, deparaffinized sections were incubated with H&E staining solution following standard protocols. For immunofluorescence staining, cell samples, tissue sections, and CEC cell sheets were permeabilized with 0.3% Triton X-100 in PBS for 15 minutes and blocked with 3% BSA in PBS for at least 1 hour at room temperature. All samples were treated with specific primary antibodies, which were diluted in 3% BSA. The sections were incubated overnight at 4°C, followed by washing with 1 × PBS for 5 minutes four times. The secondary antibodies were diluted in 3% BSA and incubated for 2 hours at room temperature. After washing with 1 × PBS for 10 minutes four times, slides were stained with Hoechst for 30 minutes. Images were taken using a ZEISS LSM 800 confocal microscope, Oberkochen, Germany or a Leica DMi8 microscope, Wetzlar, Germany. The antibody information is shown in Supplementary Table S2.

RNA Isolation and Quantitative RT-PCR

These experiments were performed with the RNeasy kit (Tiangen, Beijing, China; cat. DP451). Total RNA were converted into cDNA using the PrimeScript RT Master Mix Kit (Takara Biotechnology, Kyoto, Japan; cat. HRR036A). For quantitative RT-PCR, the reaction solution contained sample cDNA, specific primers, and iTaq Universal SYBR Green Supermix kit (Bio-Rad Life Science, Hercules, CA, USA; cat.

Investigative Ophthalmology & Visual Science

1708880). The reactions were performed in a QuantStudio 7 Flex system (Life Technologies, Singapore City, Singapore). The experiment data analysis was normalized by GAPDH. All reactions were performed in triplicates. The sequence information of all primers is shown in Supplementary Table S3.

Lentiviral Vectors and Gene Knockdown Experiments

Short hairpin RNAs (shRNAs) targeting *PAX6* and *WNK2* were designed and inserted into the PLKO.1 plasmid, respectively. Two individual shRNA sequences were designed for each gene in this study and used separately. A *scramble* shRNA without a specific targeting sequence was used as the negative control in this study. After the lentivirus package, LSCs were infected for 36 hours with 8 µg/mL polybrene in LSC culture medium. Puromycin (2 µg/mL) was used for 2 days to ensure the selection of positive infected cells. After selection, the medium was switched to normal LSC culture medium and changed daily until the cells reached confluence. The *scramble*-, *shPAX6*-, and *shWNK2*-transfected LSCs were further differentiated into CECs, followed by quantitative RT-PCR, immunofluorescence staining, and RNA sequencing analysis experiments. The *PAX6* and *WNK2* knockdown efficiency remained stable in both the LSC and CEC systems until collection for further experiments. All shRNA sequences are listed in Supplementary Table S4.

Western Blot Analysis

Cells were washed with cold PBS twice. Next, the total proteins of *scramble*-, *shPAX6*-, *shWNK2*-transfected CECs were lysed and extracted using RIPA Lysis buffer (Beyotime Institute of Biotechnology, Shanghai, China; cat. P0013B) with protease and phosphatase inhibitor cocktails (Thermo Fisher Scientific, Waltham, MA, USA, cat. 1861281). The protein concentration of all samples was determined by a bicinchoninic acid protein (BCA) assay kit (Thermo Fisher Scientific, Waltham, MA, USA, cat. A53226). Equal amounts of protein were loaded and electrophoresed on SDS-PAGE gels (Tsingke Biological Technology, Shanghai, China, cat. TSP024). The separated proteins were then transferred to a polyvinylidene difluoride membrane. Next, the membranes were blocked for 2 hours at room temperature with 5% BSA in Tris-buffered saline with 0.1% Tween 20 (TBST). The membranes were incubated with PAX6 (BioLegend, San Diego, California, USA, cat. 901301) and GAPDH (GeneTex Inc., Irvine, CA, USA, cat. GTX100118) antibodies overnight at 4°C. After washing with TBST for three times, the membranes were incubated for 1 hour with the appropriate secondary antibodies conjugated with HRP (Cell Signaling Technology, cat. 7074P2). A ECL reagent was used to detect the specific protein bands, and the results were photographed using a Bio-Rad detection system (Bio-Rad).

RNA Sequencing Analysis

Total RNA of LSCs, CECs, and *scramble*-, *shPAX6*-, *shWNK2*-transfected CECs were extracted as described above. RNA libraries were prepared by using the VAHTS Universal V6 RNA-seq Library Prep Kit (Illumina, San Diego, CA, USA) and sequenced on a Novaseq 6000 S4 platform (Annoroad Gene Technology Co. Ltd., Beijing, China) under the condition of a paired-end 150-read setting. For read count calculation, the sequencing reads were aligned to human genome(hg19) using the STAR (version 2.6.1a) software tool. The transcripts per million reads values (TPM) of each gene were generated by the RSEM (version v1.3.0) tool. The differential expression genes were called using DESeq2 (version 1.20.0), with a selection condition of an adjusted P value (Padj) <0.05 and log2 fold change >1. Further functional analysis, including the Gene Ontology biological process (GO BP) and Kyoto Encyclopedia of Genes and Genomes (KEGG) analysis, was generated by subjecting the differential expression genes list to the online DAVID (Database for Annotation, Visualization and Integrated Discovery) tool (https://david.ncifcrf.gov/home.jsp). The results of gene set enrichment (GSEA) analysis were generated with the KEGG gene set, and the significance threshold was an false discovery rate (FDR) q value ≤ 0.05.

The published human corneal bacterial and fungal keratitis transcriptomic data set[19] was obtained from the Gene Expression Omnibus database with number GSE58291. All data sets, including 7 corneal bacterial keratitis, 8 corneal fungal keratitis, and 12 normal cornea, were downloaded. The differential expressed genes with $P < 0.05$ (Student's t-test) in corneal bacterial or fungal keratitis versus normal cornea were deemed statistically significant. A combined analysis of the differential expressed genes (DEGs) in *shWNK2*-transfected CECs and the published corneal diseases was conducted. GO BP analysis was performed to assess the functions of these overlapping genes.

Processed DEG lists and other relevant gene lists are included in Supplementary Files 1 to 5.

Statistical Analysis

Student's t-test was used to calculate data between two groups. Each experiment was performed three times. Results are shown as mean ± SD. $P < 0.05$ was assumed to represent a statistical significance result.

Results

Potential Downstream Regulators of PAX6-Mediated CEC Differentiation Process

To further explore the downstream molecular events involved in PAX6-mediated CEC differentiation, human primary LSCs were cultured and identified by the stem cell markers p63 and KRT14.[20] These cells were also positive for PAX6 and MKI67[12,21] and negative for KRT12, ALDH3A1, and CLU (Fig. 1A). A serum-free air–liquid differentiation system was established to obtain mature CECs in vitro.[22,23] In this system, keratinocyte growth factor[24] and calcium chloride[25] were added to promote differentiation (Fig. 1C). As expected, stratified CECs were obtained using the CEC-specific markers KRT12,[26] ALDH3A1,[27] and CLU.[28] Moreover, CECs expressed PAX6 but were negative for MKI67, p63, and KRT14 (Fig. 1B). Quantitative RT-PCR was performed to confirm the expression of KRT12, ALDH3A1, and CLU, which were highly upregulated during differentiation (Fig. 1D).

Next, we generated *shPAX6*-transfected LSCs by specifically targeting *PAX6* short hairpin RNA (*shPAX6*), which were then differentiated into *PAX6*-depleted CECs. RNA sequencing (RNA-seq) analysis showed that 437 downregulated genes upon *PAX6* depletion were involved in differentiation (Fig. 1E, Supplementary File 4; adjusted $P < 0.05$). The RNA-seq analysis results were derived from two biological

Investigative Ophthalmology & Visual Science

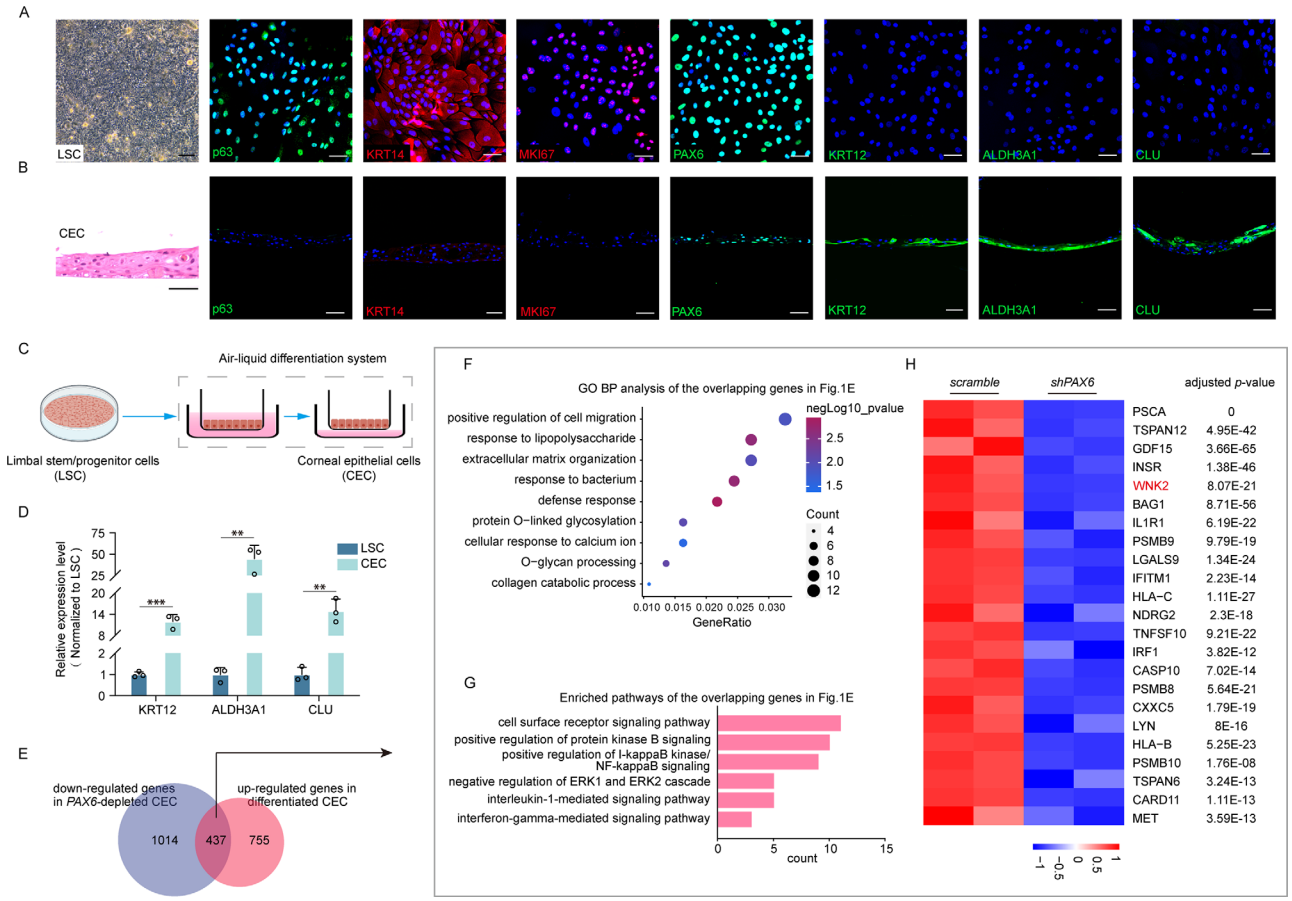

Figure 1. LSC and CEC culture systems and RNA-seq analyzed the potential downstream effector of PAX6-mediated CEC differentiation. (**A**) Phase-contrast image of cultured LSCs (*left*). Immunostaining images of p63, KRT14, PAX6, MKI67, KRT12, ALDH3A1, and CLU in primary cultured LSCs. (**B**) H&E staining image of air–liquid differentiated CECs (*left*). Immunostaining images of the indicated marker genes in differentiated mature CECs. Immunostaining and H&E staining images (*scale bar:* 50 µm); phase-contrast image (*scale bar*: 200 µm). (**C**) The graphic illustrates the differentiation process of LSC-derived CECs within an air–liquid interface system. This graphic was created with BioGDP.com. (**D**) Quantification of *KRT12*, *ALDH3A1*, and *CLU* expression level in CECs versus LSCs. (**E**) Venn diagram displays the overlap between downregulated genes in *PAX6*-depleted CECs and genes preferentially expressed in differentiated CECs. The upregulated genes in differentiated CEC are shown in Supplementary File 1. The downregulated genes in *PAX6*-depleted CEC are shown in Supplementary File 2. The overlapping genes are shown in Supplementary File 4. (**F**) GO BP enrichment analysis of the overlapping genes in E. (**G**) Enriched pathways of the overlapping genes in E based on GO analysis. (**H**) Heatmap showing the gene expression data in signaling pathways with comparison of *shPAX6*-transfected CECs and their control. (Two biological samples of each group were used. Genes were sorted by the log2 fold change with adjusted $P < 0.05$.) $^{**}P < 0.01$, $^{***}P < 0.001$.

replicates in each group. Among these 437 differentiation-associated genes, we first focused on the genes with top 20 adjusted *P* values upon *PAX6* depletion (Supplementary File 4). After excluding genes previously reported to regulate corneal epithelial cell functions, BCAS1 was selected for further investigation. However, after quantitative RT-PCR validation, knockdown of *BCAS1* showed no impact on CEC differentiation (Supplementary Fig. S1A). Consequently, we concentrated on the functional analysis of these 437 genes. GO BP enrichment analysis revealed that these genes were mainly enriched in positive regulation of cell migration, extracellular matrix organization, protein O-linked glycosylation, O-glycan processing, cellular response to calcium ions, and collagen catabolic processes (Fig. 1F). Next, we analyzed the signaling pathways that might be activated by these coregulated gene sets. We noticed that several signaling pathways were affected in *PAX6*-depleted CECs, including the cell surface receptor, protein kinase B, I-kappaB kinase/NF-kappaB, ERK1 and ERK2 cascades, interleukin-1–mediated pathway, and interferon-gamma–mediated signaling pathways (Fig. 1G). After excluding genes with low expression levels (TPM < 10), the downregulated genes among these pathways were sorted by log2 fold change in *shPAX6*-transfected CECs versus controls (Fig. 1H). Among them, WNK2 exhibited a large decrease upon *PAX6* depletion and was chosen for subsequent analyses.

WNK2 Acts as a Downstream Target of PAX6 in CEC Differentiation

We validated the WNK2 expression pattern in corneal epithelial cells both in vitro and in vivo. We found that the mRNA expression levels of *PAX6* and *WNK2* increased 13.4- and 16.3-fold, respectively, in CECs compared to those in LSCs (Fig. 2A). The differentiated cells exhibited strong PAX6 and WNK2 expression (Fig. 2B). However, WNK2 was only weakly expressed in the nucleus and barely expressed in the cytosol and plasma membrane of LSCs (Fig. 2C). In adult human limbus–corneal tissues, PAX6-positive cells were located in all epithelial layers, including the cornea

Investigative Ophthalmology & Visual Science

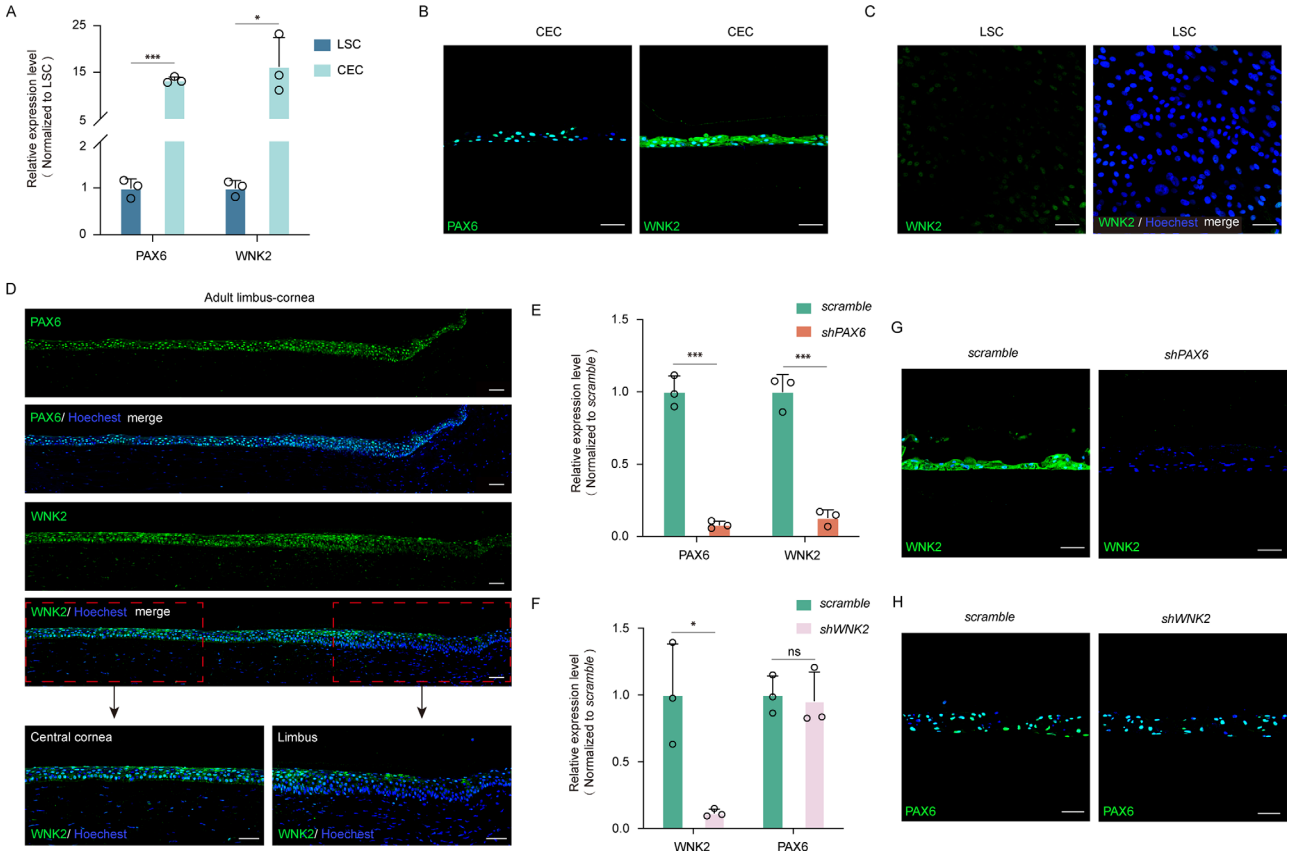

Figure 2. WNK2 might act as a downstream regulator of PAX6 in the CEC differentiation process. (**A**) Quantification of *PAX6* and *WNK2* expression level in CECs versus LSCs. (**B**) Immunostaining images showing the expression of PAX6 and WNK2 in differentiated CECs. (**C**) Immunostaining images showing the expression of WNK2 in LSCs. (**D**) Immunostaining images showing the expression of PAX6 and WNK2 in adult human corneal–limbus tissues. (**E**, **F**) Quantification of *PAX6* and *WNK2* expression levels in *scramble*-, *shPAX6*-, and *shWNK2*-transfected CECs. (**G**, **H**) Immunofluorescence staining for PAX6 and WNK2 in *scramble*-, *shPAX6*-, and *shWNK2*-transfected CECs. *Scale bar*: 50 µm. $^{*}P < 0.05$, $^{***}P < 0.001$.

and limbus. Unlike PAX6, the distribution of WNK2 was limited to the corneal epithelium and suprabasal epithelial cells of the limbus, and it was barely detected in the limbal basal epithelium (Fig. 2D), consistent with the in vitro findings.

To confirm the relationship between PAX6 and WNK2, we generated *shWNK2*-transfected LSCs. Quantitative RT-PCR and immunofluorescence staining were performed to detect the alterations in PAX6 and WNK2 expression upon differentiation. The mRNA expression level of *WNK2* decreased upon *PAX6* depletion (Fig. 2E), whereas the depletion of *WNK2* had no impact on *PAX6* expression (Fig. 2F). Consistent with quantitative RT-PCR results, immunofluorescence staining revealed that WNK2 expression was suppressed in *shPAX6*-transfected CECs (Fig. 2G), while the *shWNK2*-transfected CECs were still positive for PAX6 (Fig. 2H). Western blot analysis also confirmed that the knockdown of *WNK2* had no effect on PAX6 expression in CECs (Supplementary Fig. S2A). Therefore, these results suggest that WNK2 acts as a downstream effector of PAX6 in CECs.

PAX6–WNK2 Axis Regulates Corneal Epithelial Differentiation and Homeostasis

To assess the function of WNK2 in CECs, RNA-seq was performed on *scramble*- and *shWNK2*-transfected LSCs in a differentiation culture system. Although there were no significant morphologic changes in *WNK2*-depleted LSCs and CECs compared with those in the *scramble*-transfected group (Fig. 3A), GSEA analysis revealed the activation of cell proliferation–related pathways in *shWNK2*-transfected CECs, including the cell cycle, JAK STAT signaling pathway, MAPK signaling pathway, and WNT signaling pathway (Fig. 3B). The GO BP results showed that the genes downregulated in *WNK2*-depleted CECs were mainly enriched in extracellular matrix organization, cellular response to calcium ions, positive regulation of cell substrate adhesion, and O-glycan processing (Fig. 3C). RNA-seq analysis revealed that depletion of *WNK2* decreased the expression of CEC-specific markers *KRT12*, *ALDH3A1*, and *CLU* (Figs. 3D, 3E). On the basis of these findings, we experimentally verified the alterations in CEC-specific markers upon *WNK2* depletion. Quantitative RT-PCR and immunofluorescence staining results revealed that *WNK2* knockdown resulted in a significant decrease in both the mRNA and protein expression levels of KRT12, ALDH3A1, and CLU in CECs (Figs. 3F, 3G). These findings support the role for WNK2 in promoting CEC differentiation and suppressing cell proliferation.

Given the similar functions of PAX6 and WNK2 in CEC differentiation, we further clarified the regulatory functions of PAX6 and WNK2 in CECs at the transcriptome level (Supplementary Files 2 and 3). We identified 196 co-descending genes in *shPAX6*- and *shWNK2*-transfected CECs

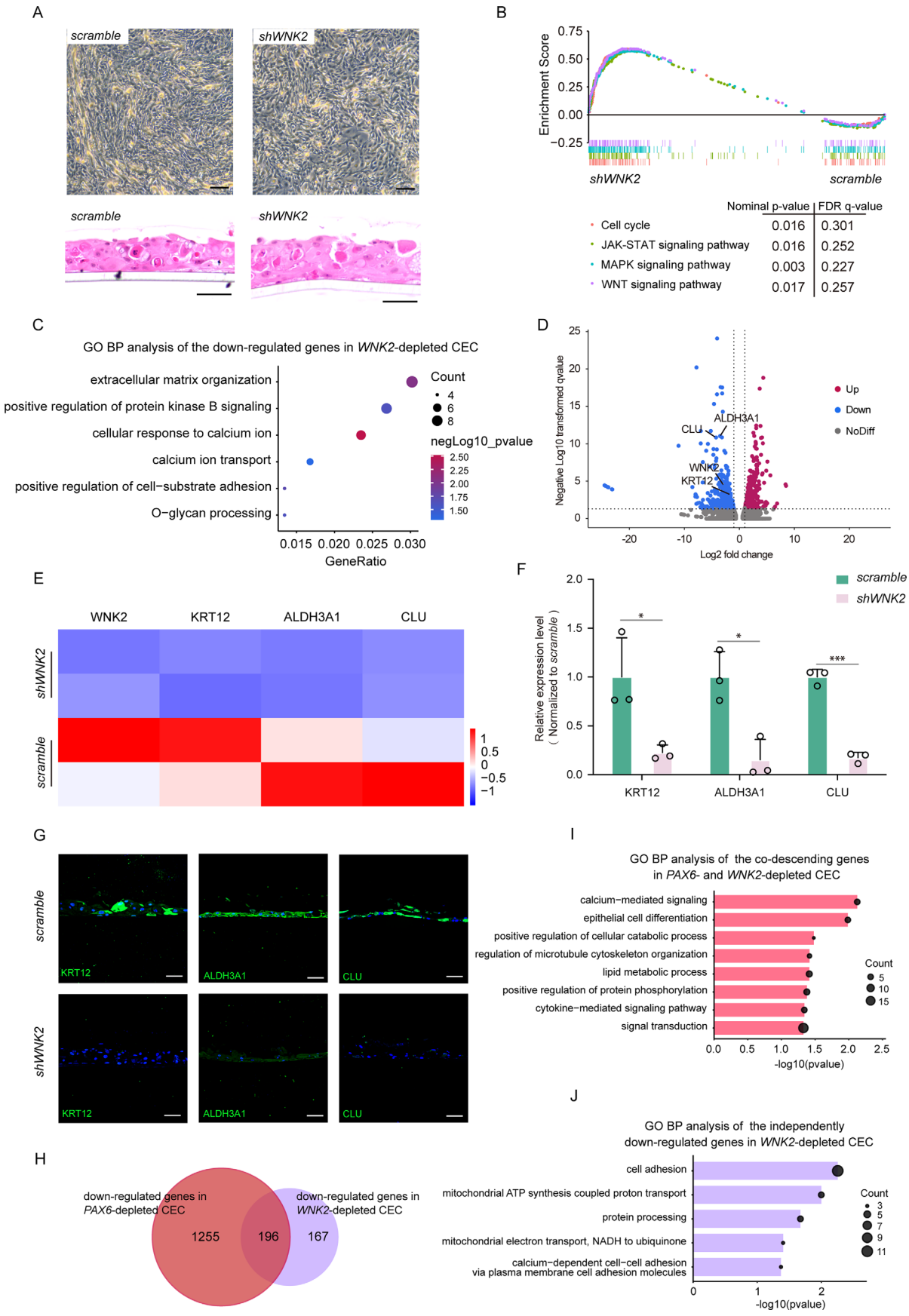

Figure 3. WNK2 participated in CEC differentiation and suppressed CEC proliferation. (**A**) Phase-contrast image (*upper*) of *scramble*- and *shWNK2*-transfected LSCs. *Scale bars*: 200 µm. H&E staining (*lower*) of *scramble*- and *shWNK2*-transfected CECs. *Scale bars*: 50 µm. (**B**) Gene set enrichment analysis showing the enriched proliferation-related KEGG pathways in *shWNK2*-transfected CECs versus the control.

(**C**) GO BP analysis showing the enriched terms of the downregulated genes in *shWNK2*-transfected CECs versus the control. (**D**) Volcano plot of the differential expression genes in *shWNK2*-transfected CECs versus the control. (**E**) Heatmap showing the gene expression of *WNK2* and CEC-specific markers in *scramble*- and *shWNK2*-transfected CECs. (**F**) Quantification of *KRT12*, *ALDH3A1*, and *CLU* expression levels in *scramble*- and *shWNK2*-transfected CECs. (**G**) Immunostaining images of KRT12, ALDH3A1, and CLU in *shWNK2*-transfected CECs and the control. *Scale bars*: 50 µm. (**H**) Overlapping of the downregulated genes in *PAX6*-depleted CECs and *WNK2*-depleted CECs. (**I**) GO BP analysis of the co-descending genes in *shPAX6*- and *shWNK2*-transfected CECs. (**J**) GO BP analysis of the independently downregulated genes in *shWNK2*-transfected CECs. $^{*}P < 0.05$, $^{***}P < 0.001$. The downregulated genes in *PAX6*-depleted and *WNK2*-depleted CECs are shown in Supplementary Files 2 and 3, respectively.

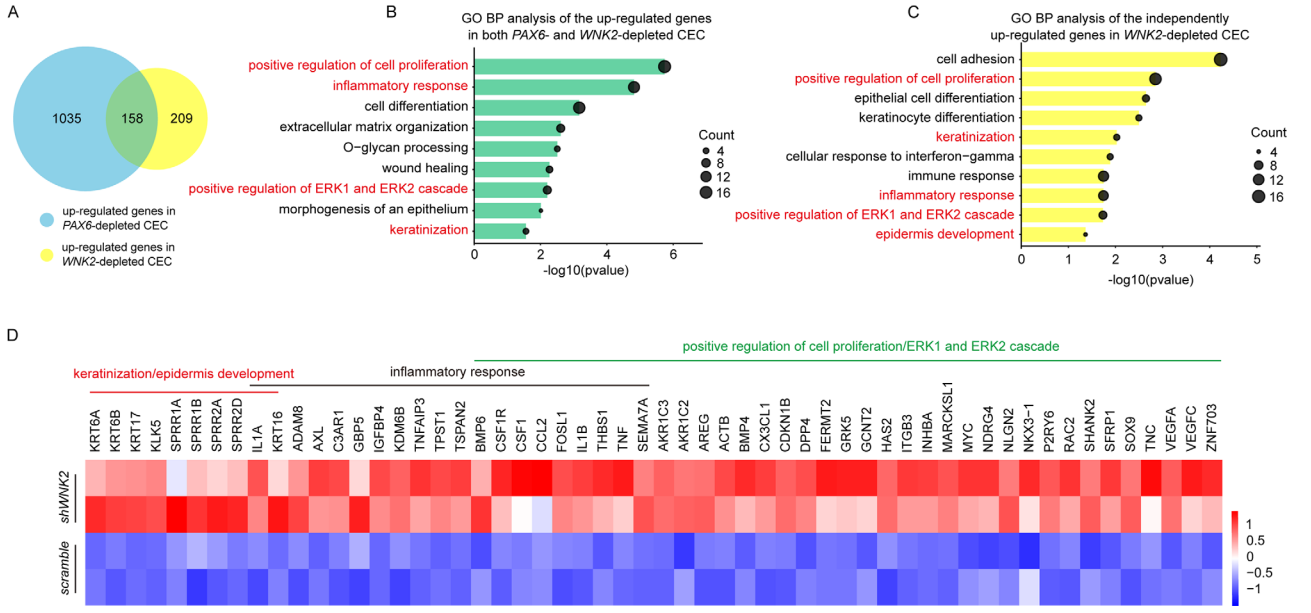

Figure 4. PAX6–WNK2 axis sustained corneal homeostasis. (**A**) Overlapping of the upregulated genes in *PAX6*-depleted CECs and *WNK2*-depleted CECs. (**B**) GO BP analysis of the upregulated genes in both *shPAX6*- and *shWNK2*-transfected CECs. (**C**) GO BP analysis of the independently upregulated genes in *shWNK2*-transfected CECs. (**D**) Heatmap showing the enriched genes in selected biological terms in *scramble*- and *shWNK2*-transfected CECs. The upregulated genes in *PAX6*-depleted and *WNK2*-depleted CECs are shown in Supplementary Files 2 and 3, respectively.

and 167 independently downregulated genes in *shWNK2*-transfected CECs (Fig. 3H). As expected, GO BP analysis of these two gene sets revealed that both genes were enriched in cell differentiation–related biological terms, including calcium-mediated signaling, epithelial cell differentiation, lipid metabolic processes, and cell adhesion processes (Figs. 3I, 3J), highlighting the importance of the PAX6–WNK2 axis in regulating CEC differentiation.

To investigate the role of WNK2 in corneal homeostasis, we focused on the upregulated gene sets in both *PAX6*- and *WNK2*-depleted CECs. We identified 158 upregulated genes that were coregulated by both PAX6 and WNK2, as well as 209 independently upregulated genes in *WNK2*-depleted CECs (Fig. 4A). GO BP analysis was also performed to analyze the two gene sets. Consistent with our findings, these upregulated genes were enriched in cell proliferation–related terms, such as positive regulation of cell proliferation or the ERK1/ERK2 cascade. Additionally, these genes were enriched in keratinization, epidermis development, and inflammatory response terms (Figs. 4B, 4C). Depletion of *WNK2* activated genes related to keratinization/epidermis development (*KRT6A*, *KRT6B*, *KRT16*, *KRT17*, *KLK5*, and *SPRRs*),[29–31] inflammatory responses (*IL1A*, *IL1B*, *CCL2*, *TNF*),[32–34] and cell proliferation (*FOSL1*, *SOX9*, *MYC*)[35–37] (Fig. 4D), suggesting a disruption of corneal homeostasis upon *WNK2* suppression. Taken together, these findings indicated that the PAX6–WNK2 axis played an essential role in maintaining corneal epithelial differentiation and corneal homeostasis.

Loss of WNK2 is Linked to Corneal Diseases

Considering the essential role of the PAX6–WNK2 axis in maintaining corneal homeostasis, we next analyzed the potential relationship between WNK2 and corneal diseases. A combined analysis of the published human corneal bacterial and fungal keratitis transcriptomic data set from the Gene Expression Omnibus database and the transcriptomic data of *shWNK2*-transfected CECs was performed to explore the potential functions of WNK2 in corneal diseases. We observed that the gene expression level of *WNK2* decreased in both corneal bacterial and fungal keratitis tissues compared to that in normal corneas ($P < 0.001$), in line with *PAX6*, *KRT12*, and *ALDH3A1* (Fig. 5A). This suggests that the aberrant expression of WNK2 may be associated with corneal diseases. Therefore, we further analyzed the coregulated genes in *WNK2*-depleted CECs and corneal diseases ($P < 0.05$). We identified 99 downregulated genes in both *WNK2*-depleted CECs and corneal diseases, including *KRT12* and *ALDH3A1* (Fig. 5B). GO BP analysis showed that these co-descending genes were also enriched in corneal differentiation and homeostasis

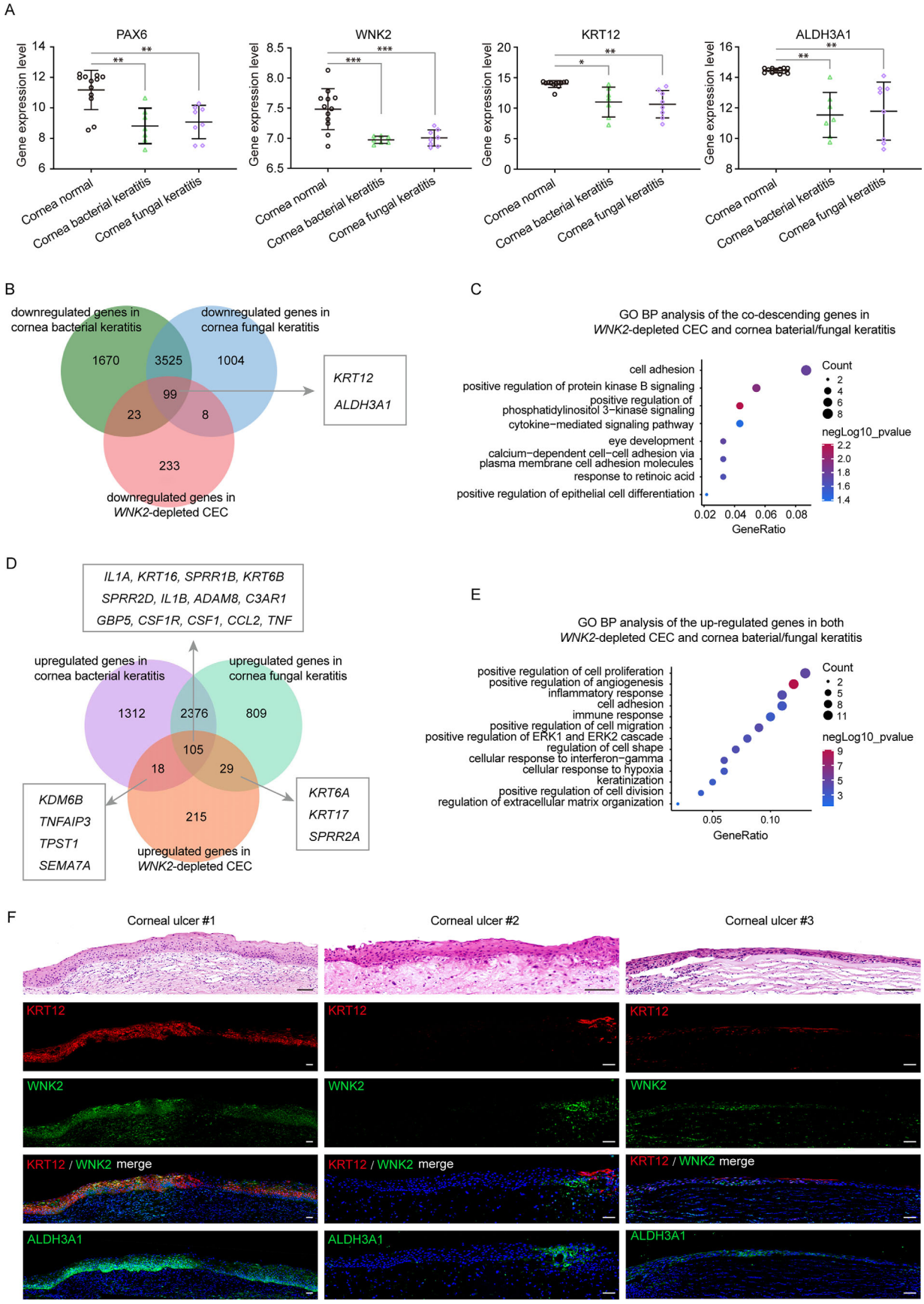

Figure 5. Loss of expression of WNK2 disrupted corneal homeostasis and was associated with corneal diseases. (**A**) The gene expression of *PAX6*, *WNK2*, *KRT12*, and *ALDH3A1* in published normal cornea and corneal bacterial/fungal keratitis. (**B**) Overlapping of the downregulated genes in corneal bacterial keratitis, corneal fungal keratitis, and *WNK2*-depleted CECs. (**C**) GO BP analysis of the downregulated genes

Investigative Ophthalmology & Visual Science

common in corneal bacterial keratitis, corneal fungal keratitis, and *WNK2*-depleted CECs. (**D**) Overlapping of the upregulated genes in corneal bacterial keratitis, corneal fungal keratitis, and *WNK2*-depleted CECs. (**E**) GO BP analysis of the upregulated genes common in corneal bacterial keratitis, corneal fungal keratitis, and *WNK2*-depleted CECs. (**F**) H&E staining and immunofluorescence staining for WNK2, KRT12, and ALDH3A1 in adult human corneal ulcer sections. The overlapping genes (**B**, **D**) are shown in Supplementary File 5. *Scale bars*: 50 µm (immunostaining images); 100 µm (H&E staining images). $^{*}P < 0.05$, $^{**}P < 0.01$, $^{***}P < 0.001$.

maintenance–associated biological terms, including positive regulation of epithelial cell differentiation, cell adhesion, calcium-dependent cell–cell adhesion, and eye development (Fig. 5C). Moreover, 152 genes were upregulated upon *WNK2* depletion and corneal diseases, including 105 genes in the three gene sets, 18 genes in *WNK2*-depleted CECs and corneal bacterial keratitis, and 29 genes in *WNK2*-depleted CECs and corneal fungal keratitis. Consistent with the above findings, we also observed the activation of keratinization-related genes (e.g., *KRT6A*, *KRT16*, *KRT17*, *SPRRs*) and inflammation-related genes (e.g., *IL1A*, *IL1B*, *TNF*, *CSF1*, *CCL2*, *ADAM8*, *SEMA7A*)[38–40] in upregulated gene sets of *WNK2*-depleted CECs and corneal diseases (Figs. 5D, 5E), confirming the regulatory role of the PAX6–WNK2 axis in maintaining corneal homeostasis.

Next, we experimentally validated our findings by performing H&E staining and immunofluorescence staining of human corneal ulcer sections from three patients. A previous study showed that the aberrant expression of PAX6 is associated with corneal ulcers.[12] As expected, lack of WNK2, KRT12, and ALDH3A1 expression was found in partial lesion areas of human corneal ulcers. In contrast, WNK2-, KRT12-, and ALDH3A1-positive cells were distributed in adjacent normal corneal tissues (Fig. 5F). These experimental findings support the important role of the PAX6–WNK2 axis in the cornea and indicate that abnormal WNK2 expression is associated with corneal diseases.

Discussion

Differentiation of lineage-committed adult somatic stem cells is essential for maintaining tissue function and homeostasis.[41,42] In this study, we identified WNK2 as a downstream target of PAX6 and uncovered the potential role of the PAX6–WNK2 axis in maintaining corneal homeostasis. Loss of expression of WNK2 disrupts corneal homeostasis, and it is associated with corneal diseases by showing similar gene and protein expression patterns. Therefore, our study provides a deeper understanding of the molecular events downstream of PAX6 in the corneal epithelium.

Most previous studies have focused on the regulators of cell fate determination in corneal epithelium. Among these studies, Dkk2 was reported to govern corneal cell fate determination. Dkk2 is expressed in the periocular mesenchyme at E11.5 and in the mesenchyme at E14.5, and it contributes in specifying the phenotype of corneal epithelium via bidirectional signaling between stromal and epithelial cells.[43] Appropriate differentiation is essential for LSCs to govern corneal homeostasis and cell identity. However, little is known about the complex downstream regulatory network involved in corneal differentiation and the maintenance of cell identity. In our previous study, PAX6 has been reported to govern fate determination and differentiation of LSCs. In this study, we focused on the downstream molecular events and identified WNK2 as a downstream target of PAX6 in corneal differentiation and maintenance of corneal homeostasis by regulating the expression of the corneal-specific markers KRT12, ALDH3A1, and CLU. Depletion of *WNK2* induced the activation of keratinization-related genes *KRT6A*, *KRT6B*, *KRT16*, *KRT17*, and *SPRRs* and inflammation-related genes *IL1A*, *IL1B*, *CCL2*, and *TNF*. Therefore, the PAX6–WNK2 axis may be a potential target for future corneal clinical treatment.

WNK2, an inhibitor of the ERK1/2 pathway,[44,45] was reported to be a tumor suppressor. Previous studies revealed that WNK2 was predominantly located in the cytoplasm,[15] while it is also suggested that this protein could be found in the plasma membrane and nucleus of colon cancer cells in recent data analysis,[46] which is consistent with current observation in corneal epithelial cells. Downregulation or loss of the WNK2 copy number has been detected in various tumor cells, including hepatocellular carcinoma, pancreatic ductal adenocarcinoma, and glial tumors.[13,44,47] WNK2 inhibits the proliferation of these tumor cells. However, the function of WNK2 in corneal epithelium remains unknown. Epithelial cells undergoing differentiation also exhibit a decline in growth ability. Therefore, we speculated that WNK2 may participate in regulating corneal epithelial differentiation. CECs with *WNK2* depletion had an epithelial-like morphology, but they were found to no longer express the CEC-specific markers. This suggested that WNK2 is essential for maintaining corneal epithelial properties of CEC characteristics. Although PAX6 and WNK2 share a similar function in corneal homeostasis, the genes affected by *WNK2* depletion do not fully overlap with those upon *PAX6* inhibition. It is speculated that WNK2 is one of the downstream executors of PAX6, and it could partially fulfill the action of this master transcription factor during corneal differentiation.

Microbial keratitis, including corneal bacterial or fungal keratitis, is characterized by corneal epithelial defects and excessive inflammatory responses that result in corneal thinning, perforation, ulceration, and loss of vision.[19,48,49] In patients with microbial keratitis, Chidambaram et al.[19] reported that the corneal epithelium–specific keratins *KRT3* and *KRT12* were downregulated while *KRT6B* and *KRT16* were upregulated, suggesting that microbial keratitis resulted in the destruction of corneal homeostasis. Previous studies also revealed that the aberrant expression of PAX6 or FOXC1, key regulators of corneal epithelial cell fate commitment, is associated with corneal disease.[50] Thus, we determined the expression of WNK2 in published corneal diseases and analyzed the coregulated genes in both *WNK2*-depleted CECs and corneal bacterial/fungal keratitis. Consistent with previous studies, our study revealed similar expression patterns of WNK2, KRT12, and ALDH3A1 in pathological corneas. *WNK2* depletion reduced the expression of corneal differentiation–related genes and activated keratinization- or inflammatory response–related genes. Moreover, we identified that the aberrant expression of WNK2 is associated with corneal ulcers, in line with K12 and ALDH3A1. Furthermore, genes that are downregulated upon *WNK2* depletion in CECs, including AQP5, NTN1, ANGPTL7, S100A8, and PLTP, have been reported to be associated with corneal diseases. Aquaporin 5 (AQP5), a regulator of corneal epithelial cell fate, plays an important role

Investigative Ophthalmology & Visual Science

in governing corneal epithelial function and homeostasis. Loss of AQP5 disrupts corneal homeostasis, as evidenced by decreased expression of KRT12 and increased expression of skin epithelial marker KRT1.[51] Netrin 1 (NTN1),[52] angiopoietin-like 7 (ANGPTL7),[53] and S100A8[54] are important regulators of corneal inflammation or neovascularization. Phospholipid transfer protein deficiency is associated with dry eye symptoms.[55] These findings provide evidence for a possible link between WNK2 and corneal diseases. Taken together, our results indicate that the PAX6–WNK2 axis plays a vital role in corneal differentiation and homeostasis.

Acknowledgments

Supported by National Natural Science Foundation of China (Grant 82271043; HO), National Natural Science Foundation of China (Grant 82301170; LZ); Guangdong Basic and Applied Basic Research Foundation (Grant 2021A1515111182; LZ), and National Natural Science Foundation of China (Grant 82171015; JY).

RNA sequencing data are available through the Gene Expression Omnibus (accession number GSE272034). Processed DEG lists are included in the supplementary files, the details of which are described in this article.

Disclosure: **L. Zhu**, None; **C. Chen**, None; **S. Wu**, None; **H. Guo**, None; **L. Li**, None; **L. Wang**, None; **D. Liu**, None; **Y. Zhan**, None; **X. Du**, None; **J. Liu**, None; **J. Tan**, None; **Y. Huang**, None; **K. Mo**, None; **X. Lan**, None; **H. Ouyang**, None; **J. Yuan**, None; **X. Chen**, None; **J. Ji**, None

References

1. Guo ZH, Zhang W, Jia YYS, Liu QX, Li ZF, Lin JS. An insight into the difficulties in the discovery of specific biomarkers of limbal stem cells. *Int J Mol Sci*. 2018;19:1982.
2. Spaniol K, Witt J, Mertsch S, Borrelli M, Geerling G, Schrader S. Generation and characterisation of decellularised human corneal limbus. *Graefes Arch Clin Exp Ophthalmol*. 2018;256:547–557.
3. Tseng SC. Concept and application of limbal stem cells. *Eye (Lond)*. 1989;3(pt 2):141–157.
4. Ho TC, Chen SL, Wu JY, et al. PEDF promotes self-renewal of limbal stem cell and accelerates corneal epithelial wound healing. *Stem Cells*. 2013;31:1775–1784.
5. Yazdanpanah G, Jabbehdari S, Djalilian AR. Limbal and corneal epithelial homeostasis. *Curr Opin Ophthalmol*. 2017;28:348–354.
6. Lobo EP, Delic NC, Richardson A, et al. Self-organized centripetal movement of corneal epithelium in the absence of external cues. *Nat Commun*. 2016;7:12388.
7. Bonnet C, Gonzalez S, Roberts JS, et al. Human limbal epithelial stem cell regulation, bioengineering and function. *Prog Retin Eye Res*. 2021;85:100956.
8. Jackson CJ, Myklebust Erno IT, Ringstad H, Tonseth KA, Dartt DA, Utheim TP. Simple limbal epithelial transplantation: current status and future perspectives. *Stem Cells Transl Med*. 2020;9:316–327.
9. Davis-Silberman N, Kalich T, Oron-Karni V, et al. Genetic dissection of Pax6 dosage requirements in the developing mouse eye. *Hum Mol Genet*. 2005;14:2265–2276.
10. Li W, Chen YT, Hayashida Y, et al. Down-regulation of Pax6 is associated with abnormal differentiation of corneal epithelial cells in severe ocular surface diseases. *J Pathol*. 2008;214:114–122.
11. Garcia-Villegas R, Escamilla J, Sanchez-Guzman E, et al. Pax-6 is expressed early in the differentiation of a corneal epithelial model system. *J Cell Physiol*. 2009;220:348–356.
12. Ouyang H, Xue Y, Lin Y, et al. WNT7A and PAX6 define corneal epithelium homeostasis and pathogenesis. *Nature*. 2014;511:358–361.
13. Dutruel C, Bergmann F, Rooman I, et al. Early epigenetic downregulation of WNK2 kinase during pancreatic ductal adenocarcinoma development. *Oncogene*. 2014;33:3401–3410.
14. Li F, Liang Z, Jia Y, et al. microRNA-324-3p suppresses the aggressive ovarian cancer by targeting WNK2/RAS pathway. *Bioengineered*. 2022;13:12030–12044.
15. Moniz S, Verissimo F, Matos P, et al. Protein kinase WNK2 inhibits cell proliferation by negatively modulating the activation of MEK1/ERK1/2. *Oncogene*. 2007;26:6071–6081.
16. Moniz S, Matos P, Jordan P. WNK2 modulates MEK1 activity through the Rho GTPase pathway. *Cell Signal*. 2008;20:1762–1768.
17. Rinehart J, Vazquez N, Kahle KT, et al. WNK2 kinase is a novel regulator of essential neuronal cation-chloride cotransporters. *J Biol Chem*. 2011;286:30171–30180.
18. Guo S, Liang Y, Murphy SF, et al. A rapid and high content assay that measures cyto-ID-stained autophagic compartments and estimates autophagy flux with potential clinical applications. *Autophagy*. 2015;11:560–572.
19. Chidambaram JD, Kannambath S, Srikanthi P, et al. Persistence of innate immune pathways in late stage human bacterial and fungal keratitis: results from a comparative transcriptome analysis. *Front Cell Infect Microbiol*. 2017;7:193.
20. Bonnet C, Gonzalez S, Deng SX, Zheng JJ. Wnt activation as a potential therapeutic approach to treat partial limbal stem cell deficiency. *Sci Rep*. 2023;13:15670.
21. Li M, Huang H, Li L, et al. Core transcription regulatory circuitry orchestrates corneal epithelial homeostasis. *Nat Commun*. 2021;12:420.
22. Zhu L, Zhang W, Zhu J, et al. Cotransplantation of limbal epithelial and stromal cells for ocular surface reconstruction. *Ophthalmol Sci*. 2022;2:100148.
23. Gonzalez S, Halabi M, Ju D, Tsai M, Deng SX. Role of Jagged1-mediated Notch signaling activation in the differentiation and stratification of the human limbal epithelium. *Cells*. 2020;9:1945.
24. Yoshihara M, Sasamoto Y, Hayashi R, et al. High-resolution promoter map of human limbal epithelial cells cultured with keratinocyte growth factor and rho kinase inhibitor. *Sci Rep*. 2017;7:2845.
25. Ma XL, Liu HQ. Effect of calcium on the proliferation and differentiation of murine corneal epithelial cells in vitro. *Int J Ophthalmol*. 2011;4:247–249.
26. Kurpakus MA, Maniaci MT, Esco M. Expression of keratins K12, K4 and K14 during development of ocular surface epithelium. *Curr Eye Res*. 1994;13:805–814.
27. Koppaka V, Chen Y, Mehta G, et al. ALDH3A1 plays a functional role in maintenance of corneal epithelial homeostasis. *PLoS One*. 2016;11:e0146433.
28. Kitazawa K, Hikichi T, Nakamura T, Sotozono C, Kinoshita S, Masui S. PAX6 regulates human corneal epithelium cell identity. *Exp Eye Res*. 2017;154:30–38.
29. Gonschorek P, Zorzi A, Maric T, et al. Phage display selected cyclic peptide inhibitors of kallikrein-related peptidases 5 and 7 and their in vivo delivery to the skin. *J Med Chem*. 2022;65:9735–9749.
30. McCarthy RL, De Brito M, O'Toole E. Pachyonychia congenita: clinical features and future treatments. *Keio J Med*. 2023, doi:10.2302/kjm.2023-0012-IR.
31. Xiang M, Zhang W, Wen H, Mo L, Zhao Y, Zhan Y. Comparative transcriptome analysis of human conjunctiva between

normal and conjunctivochalasis persons by RNA sequencing. *Exp Eye Res*. 2019;184:38–47.
32. Huyghe J, Priem D, Bertrand MJM. Cell death checkpoints in the TNF pathway. *Trends Immunol*. 2023;44:628–643.
33. Galozzi P, Bindoli S, Doria A, Sfriso P. The revisited role of interleukin-1 alpha and beta in autoimmune and inflammatory disorders and in comorbidities. *Autoimmun Rev*. 2021;20:102785.
34. Dewald O, Zymek P, Winkelmann K, et al. CCL2/monocyte chemoattractant protein-1 regulates inflammatory responses critical to healing myocardial infarcts. *Circ Res*. 2005;96:881–889.
35. Zhou ZQ, Hurlin PJ. The interplay between Mad and Myc in proliferation and differentiation. *Trends Cell Biol*. 2001;11:S10–14.
36. Liu C, Liu L, Chen X, et al. Sox9 regulates self-renewal and tumorigenicity by promoting symmetrical cell division of cancer stem cells in hepatocellular carcinoma. *Hepatology*. 2016;64:117–129.
37. Vallejo A, Erice O, Entrialgo-Cadierno R, et al. FOSL1 promotes cholangiocarcinoma via transcriptional effectors that could be therapeutically targeted. *J Hepatol*. 2021;75:363–376.
38. Silvan J, Gonzalez-Tajuelo R, Vicente-Rabaneda E, et al. Deregulated PSGL-1 expression in B cells and dendritic cells may be implicated in human systemic sclerosis development. *J Invest Dermatol*. 2018;138:2123–2132.
39. Namavari A, Chaudhary S, Ozturk O, et al. Semaphorin 7a links nerve regeneration and inflammation in the cornea. *Invest Ophthalmol Vis Sci*. 2012;53:4575–4585.
40. Ueland HO, Ueland GA, Lovas K, et al. Novel inflammatory biomarkers in thyroid eye disease. *Eur J Endocrinol*. 2022;187:293–300.
41. Won JH, Choi JS, Jun JI. CCN1 interacts with integrins to regulate intestinal stem cell proliferation and differentiation. *Nat Commun*. 2022;13:3117.
42. Ljubimov AV, Saghizadeh M. Progress in corneal wound healing. *Prog Retin Eye Res*. 2015;49:17–45.
43. Walker H, Akula M, West-Mays JA. Corneal development: role of the periocular mesenchyme and bi-directional signaling. *Exp Eye Res*. 2020;201:108231.
44. Zhou SL, Zhou ZJ, Hu ZQ, et al. Genomic sequencing identifies WNK2 as a driver in hepatocellular carcinoma and a risk factor for early recurrence. *J Hepatol*. 2019;71:1152–1163.
45. Dong P, Xiong Y, Yu J, et al. Control of PD-L1 expression by miR-140/142/340/383 and oncogenic activation of the OCT4-miR-18a pathway in cervical cancer. *Oncogene*. 2018;37:5257–5268.
46. Wu J, Meng X, Gao R, et al. Long non-coding RNA LINC00858 inhibits colon cancer cell apoptosis, autophagy, and senescence by activating WNK2 promoter methylation. *Exp Cell Res*. 2020;396:112214.
47. Hong C, Moorefield KS, Jun P, et al. Epigenome scans and cancer genome sequencing converge on WNK2, a kinase-independent suppressor of cell growth. *Proc Natl Acad Sci USA*. 2007;104:10974–10979.
48. Tuft S, Somerville TF, Li JO, et al. Bacterial keratitis: identifying the areas of clinical uncertainty. *Prog Retin Eye Res*. 2022;89:101031.
49. Singh RB, Zhu S, Yung A, Dohlman TH, Dana R, Yin J. Efficacy of cyanoacrylate tissue adhesive in the management of corneal thinning and perforation due to microbial keratitis. *Ocul Surf*. 2020;18:795–800.
50. Li M, Zhu L, Liu J, et al. Loss of FOXC1 contributes to the corneal epithelial fate switch and pathogenesis. *Signal Transduct Target Ther*. 2021;6:5.
51. Wang Y, Di G, Zhang K, et al. Loss of aquaporin 5 contributes to the corneal epithelial pathogenesis via Wnt/beta-catenin pathway. *FASEB J*. 2023;37:e22776.
52. Han Y, Shao Y, Lin Z, et al. Netrin-1 simultaneously suppresses corneal inflammation and neovascularization. *Invest Ophthalmol Vis Sci*. 2012;53:1285–1295.
53. Toyono T, Usui T, Yokoo S, et al. Angiopoietin-like 7 is an anti-angiogenic protein required to prevent vascularization of the cornea. *PLoS One*. 2015;10:e0116838.
54. Tong L, Lan W, Lim RR, Chaurasia SS. S100A proteins as molecular targets in the ocular surface inflammatory diseases. *Ocul Surf*. 2014;12:23–31.
55. Setala NL, Metso J, Jauhiainen M, Sajantila A, Holopainen JM. Dry eye symptoms are increased in mice deficient in phospholipid transfer protein (PLTP). *Am J Pathol*. 2011;178:2058–2065.

Investigative Ophthalmology & Visual Science